

Received June 23, 2021, accepted July 10, 2021, date of publication July 26, 2021, date of current version August 4, 2021.

Digital Object Identifier 10.1109/ACCESS.2021.3099205

# Detection of Blast Furnace Hearth Lining Erosion by Multi-Information Fusion

JIAOCHENG MA<sup>1</sup>, XUEWEI WEN<sup>1</sup>, AND XIN ZHAO<sup>2</sup>

<sup>1</sup>School of Mechanical Engineering and Automation, Northeastern University, Shenyang, Liaoning 110004, China

<sup>2</sup>Liaoning Provincial Institute of Safety Science, Shenyang 110004, China

Corresponding author: Jiaocheng Ma (majiaocheng@mail.neu.edu.cn)

This work was supported in part by the Fundamental Research Funds for the Central Universities under Grant N180304020, and in part by the National Natural Science Foundation of China under Grant 61963002.

**ABSTRACT** The blast furnace hearth refractories are exposed to complex chemical attack and thermal stress erosion, which will lead to the gradual failure of refractories. The campaign life of a blast furnace depends on its remaining hearth refractory lining, so it is very important to understand the remaining thickness of hearth refractory for prolonging the service life of blast furnace. In order to understand the damage of hearth refractory more accurately, a multi-information fusion method for measuring the refractory lining thickness of blast furnace hearth was proposed, which was based on the application advantages of impact echo technology, thermocouple and cooling stove heat flux intensity in blast furnace hearth. The influence of temperature change in different material layers of hearth on wave velocity was considered. In addition, the thickness of carbon brick lining of blast furnace hearth was detected by the method of multi-information fusion. It is found that the multi-information fusion thickness detection method improves the accuracy of thickness measurement compared with the impact echo thickness detection method.

**INDEX TERMS** Blast furnace hearth, cooling stove heat flux intensity, multi-information fusion, simulation, thermocouple, thickness detection.

## I. INTRODUCTION

The development of a country's national economy and the promotion of national defense force can't be separated from the iron and steel industry. Blast furnace is an important ironmaking equipment in iron and steel industry, and hearth plays an important role in blast furnace ironmaking. In production, the hearth can hold high temperature molten iron, and can make the smelted molten iron flow out from the tap hole normally. During the whole smelting process, the main reasons for the erosion and deterioration of hearth lining are mechanical stress, thermal stress crack and chemical attack. As time goes on, lining erosion will become more and more serious. If erosion causes the lining thickness of the hearth to be too thin, the molten iron will leak out, which will bring serious threat to the safe production of blast furnace and cause huge losses to enterprises and society. If the thickness with reference value can be detected in real time during the operation of the blast furnace, the working intensity can be adjusted or the blast furnace can be repaired in time, so as

to avoid further erosion and damage of the hearth lining and prolong the service life of the blast furnace. However, the blast furnace is a closed vessel which works continuously under high temperature and high pressure. This will bring great difficulties to the detection of the lining thickness of the blast furnace hearth.

Domestic and foreign related scholars and researchers have developed a variety of blast furnace hearth thickness measurement technologies, and have achieved certain results [1], [2]. Canadian Hatch company and scholar Afshin Sadri introduced the impact echo technology into the field of blast furnace detection, and developed it into a new technology, namely Acousto Ultrasonic-Echo (AU-E) technology. The literature [3], [4] introduced the basic principle of AU-E technology, then studied the influence of temperature, furnace shape and size on wave velocity, detected the thickness of blast furnace hearth by AU-E technology and verified by physical measurement of hearth. The literature [5], [6] studied the application of AU-E technology in blast furnace hearth, the influence of temperature on the velocity of stress wave was calculated through the carbon brick sample of blast furnace to be tested, and then the hearth lining thickness

The associate editor coordinating the review of this manuscript and approving it for publication was Giambattista Gruosso<sup>1</sup>.

TABLE 1. Material properties.

Materials	$\rho(\text{kg/m}^3)$	Thermal conductivity [W/(m <sup>2</sup> ·K)]	$T(^{\circ}\text{C})$	$E(\text{Pa})$	Coefficient of linear expansion( $\text{k}^{-1}$ )	Poisson's ratio
Shell/Sealing plate	7800	50	30	$2.06 \times 10^{11}$	$1.2 \times 10^{-5}$	0.27
			500	$1.70 \times 10^{11}$		
			1000	$0.90 \times 10^{11}$		
			1500	$0.20 \times 10^{11}$		
Filling material 1	1600	0.35	20	$2.15 \times 10^{10}$	$2.8 \times 10^{-6}$	0.15
			500	$1.50 \times 10^{10}$		
			800	$1.25 \times 10^{10}$		
Cooling stave	7570	40	With the furnace shell		$5.87 \times 10^{-6}$	0.27
Filling material 2	1600	3.6	With the filling material 1		$2.8 \times 10^{-6}$	0.15
Carbon brick	1850	10	With the filling material 1		$3.4 \times 10^{-6}$	0.15

was calculated by the wave velocity, finally, the thickness was verified by damage investigation after shut down. The literature [7]–[9] described the detection of lining thickness of several blast furnace hearth by AU-E technology, the wave velocity in the thickness calculation was determined by the refractory data sheets and mechanical properties of similar bricks, and the hearth thickness detection results were verified on the blast furnace of the same design. The literature [10], [11] used AU-E technology and thermal data from thermocouples and cooling system to calculate the lining thickness of blast furnace hearth and predict the further wear area over time. However, this method is only about the analysis of thickness results, which doesn't improve the accuracy of AU-E thickness detection. In the above hearth thickness detection, although the influence of temperature on velocity was analyzed, the wave velocity calibration of laboratory samples ignores the influence of temperature of other material layers in the hearth on the wave velocity, and query of refractory data sheets of similar bricks brings the uncertainty of wave velocity, this will lead to thickness calculation error. In order to overcome the above problems, the impact echo technology combined with thermocouple data and cooling stave heat flux intensity of a multi-information fusion detection method is applied to the blast furnace hearth thickness detection, this method considers the influence of temperature change in different material layers of the hearth on the wave velocity, and then calculates the thickness of the hearth more accurately.

II. MODELS AND METHODS  
A. FINITE ELEMENT MODEL

A 3200m<sup>3</sup> blast furnace is taken as the research object. Its design structure is shown in Fig. 1. The thickness of each layer structure of the hearth bottom is as follows. The thickness of furnace shell is 50mm, the thickness of filling material 1 between the furnace shell and the cooling stave is 60mm, the thickness of cooling stave is 120mm and the height is 1200mm, the thickness of filling material 2 between the cooling stave and the lining carbon brick is 60mm. The thickness of bottom filling material 2 is 100mm, the thickness of bottom sealing plate is 32mm. The material properties are shown in Table 1.

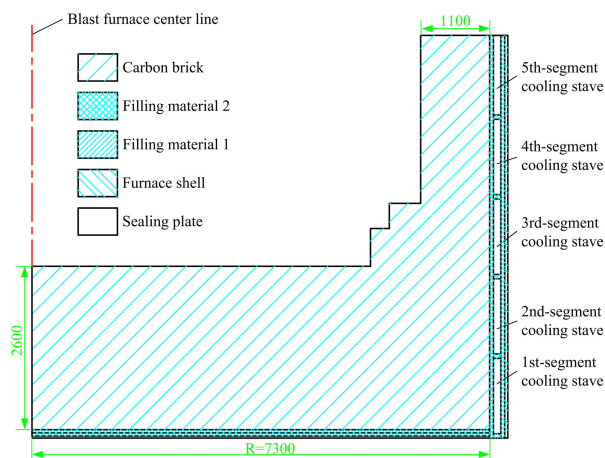


FIGURE 1. Design structure of blast furnace hearth bottom.

The cooling water pipe in the hearth cooling stave is a serpentine pipe with an inner diameter of 40mm, and the center of the water pipe is distributed on the middle surface of the cooling stave. The gap between different segments of the cooling stave is 67.5mm, and that between the same segments of the cooling stave is 62mm. Each segment has 38 cooling staves evenly distributed in the circumferential direction. The cooling water speed is 2m/s, and the ambient temperature is 25°C. The bottom cooling water pipe is located on the bottom sealing plate, and the center of the water pipe is located in the middle of bottom filling material 2, the inner diameter is 46mm, the number of water pipes is 44, the cooling water speed is 1.22m/s, and the ambient temperature is 30°C. The cooling water of hearth cooling stave and bottom is supplied by dual systems, and the soft water closed circulation cooling system is adopted.

The local design model of hearth bottom was established by finite element software, which includes two cooling staves in the circumferential direction, as shown in Fig. 2. In order to reduce the calculation amount of thickness detection on the model by the impact echo technology, according to the characteristics of impact echo thickness detection [2], the corresponding hearth of the cooling stave far from the bottom in the temperature field is intercepted as the impact echo thickness detection model.

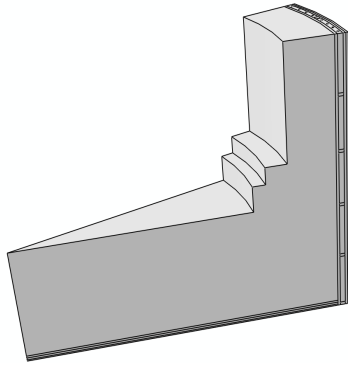


FIGURE 2. Local design model of hearth bottom.

**B. METHODS**

**1) EQUIVALENT CONVECTIVE HEAT TRANSFER COEFFICIENT AT HEARTH BOTTOM**

Under normal operation of blast furnace, the heat of the blast furnace is constantly transferred from the inside to the outside. The heat is taken away by the cooling water and the air outside the furnace shell.

According to the empirical formula [12], the convective heat transfer coefficient at the inner surface of the water pipe can be taken

$$h_w = 208.8 + 47.5 v_w W / (m^2 \cdot K) \tag{1}$$

where,  $v_w$  is the cooling water speed, m/s.

According to the wetted perimeter method [13], the equivalent convective heat transfer coefficient of the middle surface of the hearth cooling stave can be calculated

$$h_Y = \frac{NMD_G}{2r_Y} h_w \tag{2}$$

where,  $N$  is the number of cooling staves in the circumferential direction of hearth,  $M$  is the number of water pipes of single cooling stave of hearth,  $D_G$  is the inner diameter of hearth water pipes,  $r_Y$  is the radius of the middle surface of hearth cooling stave.

The equivalent convective heat transfer of water pipe at the bottom is

$$h_e = \frac{\pi N_P D_P}{d_h} h_w \tag{3}$$

where,  $N_P$  is the number of cooling water pipes at the bottom,  $D_P$  is the inner diameter of cooling water pipes at the bottom, and  $d_h$  is the diameter of hearth.

According to the single-layer cylinder structure [14], the equivalent convective heat transfer coefficient on the middle surface of the hearth cooling stave is equivalent to the cold surface of cooling stave, the equivalent convective heat transfer coefficient of the cold surface of cooling stave is  $151.8W/(m^2 \cdot K)$ . The convective heat transfer coefficient of air is  $20W/(m^2 \cdot K)$ , and the ambient temperature is  $30^\circ C$  [15]. According to formula 3, the equivalent convective heat transfer coefficient of furnace bottom is  $47.2W/(m^2 \cdot K)$ .

**2) PRINCIPLE OF THICKNESS MEASUREMENT**

Impact echo technology is a nondestructive testing technology based on transient stress wave, the stress wave is divided into P, S and R wave. The propagation direction of P-wave is the same as the vibration direction of medium particle, and P-wave speed is the fastest, so the impact echo method is mainly concerned with P-wave. The stress wave can be generated by mechanical impact or, hammer or steel ball. The test surface should be as clean and smooth as possible. The signal receiving device is located at a certain distance near the detection point, which can be a wide-band displacement sensor or an acceleration sensor.

The P-wave is captured and analyzed by the signal receiving device, the velocity of P-wave varies with the density and elasticity of the propagating material, for an isotropic material, P-wave propagation velocity is

$$V_P = \sqrt{\frac{E_0}{\rho} \frac{1 - \mu}{(1 + \mu)(1 - 2\mu)}} \tag{4}$$

where,  $E_0$  is the elastic modulus of the material at room temperature,  $\rho$  is the density of the material,  $\mu$  is the Poisson's ratio of the material [16]. The physical properties of the materials used in the hearth are essentially the same in each direction [17], so the application of equation 4 is appropriate.

When the impact echo method is used to measure the thickness of blast furnace hearth, the P-wave velocity is affected by the temperature and shape of refractory material of furnace hearth [18]. The shape factor  $\beta$  is used to correct the influence of the shape of refractory material of furnace hearth on wave velocity. For most blast furnaces, the lateral dimensions are at least six times of the hearth lining thickness, and the shape factor  $\beta$  is 0.96 [19]. Temperature factor  $\alpha$  is used to correct the influence of internal temperature of different materials in blast furnace hearth on wave velocity. The temperature factor  $\alpha$  and shape factor  $\beta$  of each layer are helpful to determine the thickness of carbon brick, because the incorrect wave velocity in the direction of the bricks installation and signal transmission will lead to wrong calculation results [5].

The temperature correction factor  $\alpha$  can be calculated by the following equation

$$\alpha = 1 + \left( \frac{\int_{T_1}^{T_2} E(T) dT}{E_0} \right) = \left( 1 + \frac{E_{d2} - E_{d1}}{E_0} \right) \tag{5}$$

where,  $T_1$  and  $T_2$  are the temperature of cold surface and hot surface of each material layer respectively,  $E_{d1}$  and  $E_{d2}$  are the elastic modulus corresponding to the cold surface and the hot surface [20].

The corrected wave velocity in the material is

$$V_{Pc} = \alpha \beta V_P \tag{6}$$

where,  $V_{Pc}$  is the corrected P-wave velocity between the cold and hot surfaces of the material [21].

At present, most blast furnace hearth is multi-layer structure. The calculation of the final refractory thickness  $H_n$  of

multi-layer hearth is based on the following equation

$$H_n = \frac{(V_p)_n \alpha_n \beta_n}{2} \left( \frac{1}{f} - \sum_{i=1}^{n-1} \frac{2H_i}{(V_p)_i \alpha_i \beta_i} \right) \quad (7)$$

where,  $f$  is the resonance frequency for the thickness of the  $n^{th}$  layer [22].

ABAQUS simulation software is used for this simulation. The following assumptions need to be made in the simulation calculation of the hearth. (1) 1150°C is the temperature value of molten iron solidification temperature, and the isotherm of 1150°C is regarded as the erosion boundary of lining carbon brick of furnace hearth [12]. (2) The heat transfer process of hearth is regarded as a steady process, and there is no heat source inside. (3) The boundary of the outer side of hearth bottom is regarded as linear and adiabatic boundary. (4) The erosion of hearth lining is uniform along the circumferential direction. (5) The tap hole is far enough away from the thickness detection position, so the influence of tap hole on the nearby temperature field is not considered in the study [15]. (6) There are no large cracks and crevices in hearth lining [23]. (7) The P-wave energy is large enough to detect the thickness of the whole lining carbon brick [24]. (8) Due to the influence of temperature, the elastic modulus of refractory changes within the uniform gradient between cold and hot surfaces [2].

### 3) CALCULATION PRINCIPLE

The initial model was established, and the material properties and convection heat transfer boundary conditions of hearth bottom were set, a 1150°C isothermal boundary was given for the hot surface of carbon brick, the temperature field was solved by steady heat transfer. According to the temperature field, the temperature factor of each material layer was calculated, and the temperature field was taken as the pre-defined field of hearth thickness detection model. The thickness of the detection model was measured by impact echo, then, a model was established based on the thickness detection results to calculate the difference between the carbon brick cold surface temperature and thermocouple temperature (or the cold surface temperature of the heat flow calculation). According to the difference, the correction direction of temperature factor was judged to be larger or smaller. The modified temperature factor model was used to continue to detect the thickness. Then the difference between the cold surface temperature of carbon brick solved by the model thickness and the thermocouple temperature (or the cold surface temperature of the heat flow calculation) was judged. This process was recycled, and finally the erosion boundary of hearth was determined. After the solution (the temperature factor met the expectation, the cold surface temperature of carbon brick solved by thickness measurement results and the thermocouple temperature (or the cold surface temperature of the heat flow calculation) were within the specified error range), the calculation results were saved, and the hearth thickness was determined. This multi-information fusion detection method could correct

the wave velocity by temperature factor, which avoided the uncertainty of the wave velocity query or the neglect of the wave velocity change of other material layers, thus the thickness error was reduced.

### C. VERIFICATION ACCURACY CONDITION

Based on the general deviation of temperature in blast furnace research, the accuracy of temperature verification is

$$\frac{|T - T_t|}{T_t} \times 100 < \varepsilon \quad (8)$$

where,  $T$  is the cold surface temperature of carbon brick under the test point solved by the thickness result of the model,  $T_t$  is the calculated temperature of thermal parameters of carbon brick cold surface,  $\varepsilon$  is the accuracy of temperature verification, and the value range is 1%-1.5%.

According to the temperature verification conditions, hearth structure and model grid unit, the step size range of temperature factor is selected as 0.002-0.018. The correction results of temperature factor should be in a certain error range with the expected value of thermal parameters calculation

$$\frac{|\alpha - \alpha_t|}{\alpha_t} \times 100 < \delta \quad (9)$$

where,  $\alpha$  is the calculated value of temperature factor of carbon brick,  $\alpha_t$  is the expected value of thermal parameter calculation,  $\delta$  is the judgment value of the temperature factor correction condition, and the value of  $\delta$  is 0.2%-0.3%.

## III. RESULTS AND DISCUSSION

In blast furnace operation, the position of erosion boundary of hearth bottom is unknown. The initial solution model can be set as the hearth bottom design prototype. The solution result of temperature field is shown in Fig.3.

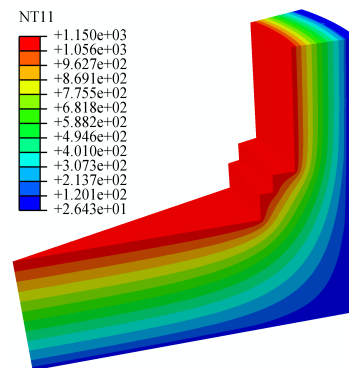


FIGURE 3. Initial temperature field.

According to the calculation of initial temperature field, the cold surface temperature of carbon brick lining was lower than that of thermocouple temperature, and the difference was large. It shows that carbon brick has been eroded to a certain extent. Therefore, in order to improve the calculation efficiency, the erosion line was moved to the cold surface for a certain distance. The temperature field results are shown in Fig. 4.

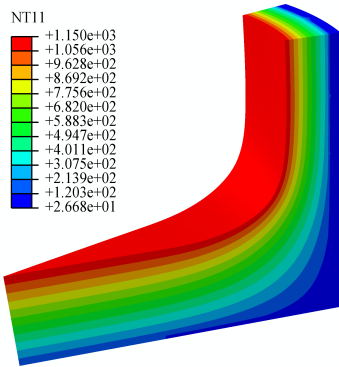


FIGURE 4. Temperature field results after erosion boundary moving.

TABLE 2. Thermocouple temperature corresponding to test point.

Test point	1	2	3	4	5	6
Temperature(°C)	380	392	409	415	388	401

TABLE 3. Temperature of each layer of blast furnace.

T(°C)	Shell	Filling material 1	Cooling stave	Filling material 2	Carbon brick
The cold surfaces	41.86	42.10	83.88	111.89	266.74
The hot surfaces	42.10	83.88	111.89	266.74	1150

**A. THICKNESS RESULTS OF IMPACT ECHO AND THERMOCOUPLE DATA**

1 to 6 in Fig. 5 are the locations of test points on the hearth, and the measured temperature of thermocouple corresponding to the test point was the highest temperature in history on the cold surface of carbon brick lining. The thermocouple temperature is shown in Table 2. The test point 1 at the hearth position in Fig.5 is taken as an example for thickness detection. Table 3 lists the node temperatures of the cold and hot surfaces of each layer materials in the temperature field model after moving the erosion line.

After fitting the relationship between temperature and elastic modulus of furnace shell and cooling stave, it is found that their internal temperature change had little effect on P-wave velocity. After fitting the relationship between temperature and elastic modulus of carbon brick and filling material, it is found that internal temperature change had a great influence on P-wave velocity. The fitting relationship of carbon brick is shown in Fig. 6.

According to equation 5, The temperature factor from furnace shell to carbon brick lining can be calculated as follows,  $\alpha_S = 1, \alpha_{FM1} = 0.974, \alpha_{CS} = 1, \alpha_{FM2} = 0.907, \alpha_{CB} = 0.566$ . The wave velocities of different material layers can be calculated according to equation 4 and 6.

The test point and signal collection point were set on the hearth model of impact echo thickness detection, and the distance between them was 100mm. As shown in figure 7, the testing time domain diagram was converted into spectrum by FFT. According to the spectrum diagram, there is an

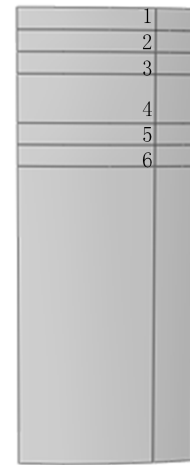


FIGURE 5. The corresponding test points under thermocouple distribution.

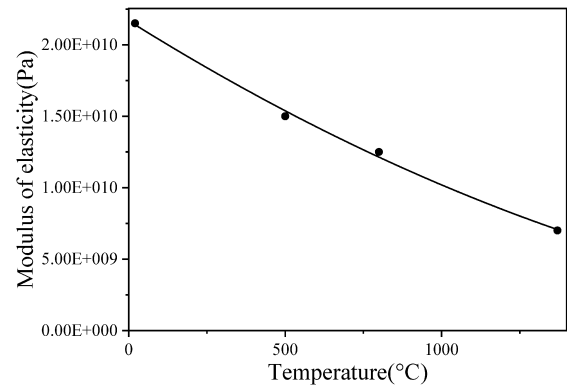


FIGURE 6. The relationship between elastic modulus and temperature of carbon brick.

obvious peak at the frequency of 949Hz, which is caused by the reflection on the inner surface of the innermost carbon brick. According to equation 7, the thickness of the carbon brick can be calculated as 875.1mm.

According to the thickness simulation analysis, the cold surface temperature of 875.1mm carbon brick was 270.43°C. The temperature difference between the cold surface temperature of carbon brick and the actual thermocouple temperature 380°C is 109.57°C. According to equation 8, the deviation is 28.83%, which is large. It can be judged that the hearth model is too thick and the temperature factor is too small. Then, according to the method of calculation principle, the thickness spectrum of test point 1 was obtained under the condition of equation 9, as shown in Fig. 8.

Fig. 8 shows an obvious peak at 1548Hz, and the thickness of carbon brick at test point 1 is 541.8mm. Based on this thickness result, the temperature field was established and the cold surface temperature of carbon brick was 380.39°C. The deviation is 0.10%. It is within the range of temperature verification accuracy. The expectation of the solved temperature factor and the convergence of the solved cold surface temperature of carbon brick and thermocouple temperature are shown in Fig. 9.

TABLE 4. Thickness results of multi-information detection.

Test point	Thickness(mm)	$\alpha$	$\alpha_t$	Temperature factor deviation (%)	$T(^{\circ}\text{C})$	$T_t(^{\circ}\text{C})$	Temperature deviation (%)
1	541.8	0.631	0.631	0.00	380.39	380	0.10
2	525.3	0.638	0.638	0.00	388.34	392	0.93
3	493.2	0.647	0.647	0.00	404.60	409	1.08
4	468.1	0.651	0.650	0.15	418.30	415	0.80
5	534.2	0.635	0.636	0.16	384.07	388	1.01
6	498.9	0.642	0.643	0.16	401.61	401	0.15

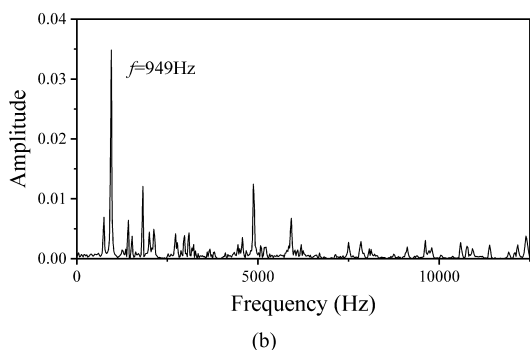
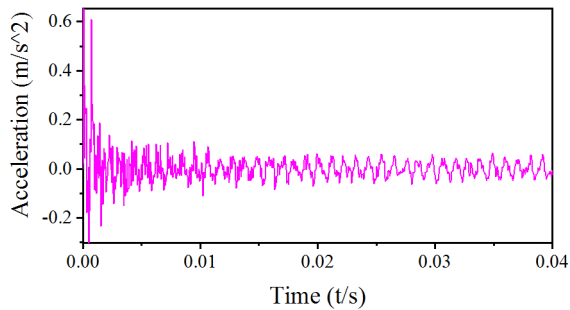


FIGURE 7. The simulation test results of carbon brick thickness.

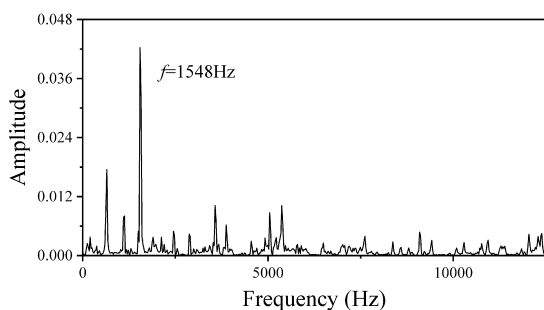


FIGURE 8. The spectrum of hearth lining thickness measurement.

According to the method of calculation principle, the thickness of carbon brick at other test points in Fig. 5 was tested. The frequency domain diagram of other test points is shown in Fig. 10. The thickness calculation results are listed in Table 4.

It can be seen from Table 4 that the maximum deviation between the cold surface temperature of carbon brick and the thermocouple temperature is 1.08%, and the minimum deviation is 0.10%, which are within the allow able deviation

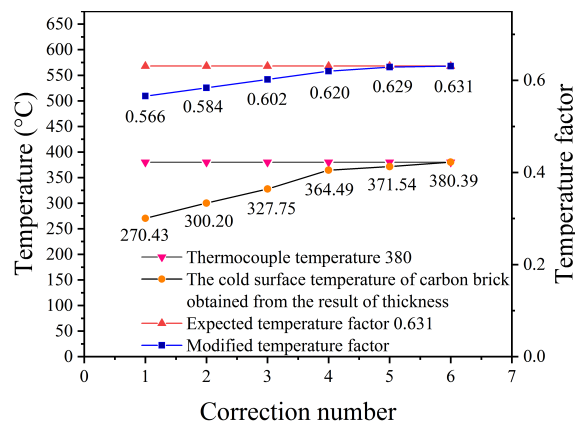


FIGURE 9. Measurement results of test point 1.

TABLE 5. Thickness results of impact echo detection.

Test point	Thickness(mm)	$T(^{\circ}\text{C})$	$T_t(^{\circ}\text{C})$	Temperature deviation(%)
1	575.9	365.52	380	3.81
2	553.5	375.40	392	4.23
3	512.6	394.91	409	3.44
4	484.9	409.33	415	1.37
5	564.5	370.48	388	4.52
6	522.3	390.10	401	2.72

range. The accuracy of simulated temperature of carbon brick cold surface is verified by thermocouple measured temperature. It is found that the thickness detection method based on multi-information fusion can accurately and effectively calculate the thickness of hearth lining carbon brick.

The influence of internal temperature of carbon brick on wave velocity was only considered in the previous impact echo detection. According to the laboratory sample detection or data table query, the wave velocity was obtained, and the thickness of the model was calculated. The same carbon brick sample was used to detect the wave velocity. The average temperature of the thermocouple was used to calculate the P-wave velocity in the sample, and the calculated propagation velocity was about 2220m/s. In this case, the thickness results and temperature deviation are shown in Table 5. The temperature deviation comparison results of Table 4 and Table 5 are shown in Fig. 11.

According to Fig. 11, it can be seen more intuitively that the temperature deviation of impact echo is larger than that of multi-information detection. Therefore, if the influence of internal temperature of carbon brick on wave velocity is only

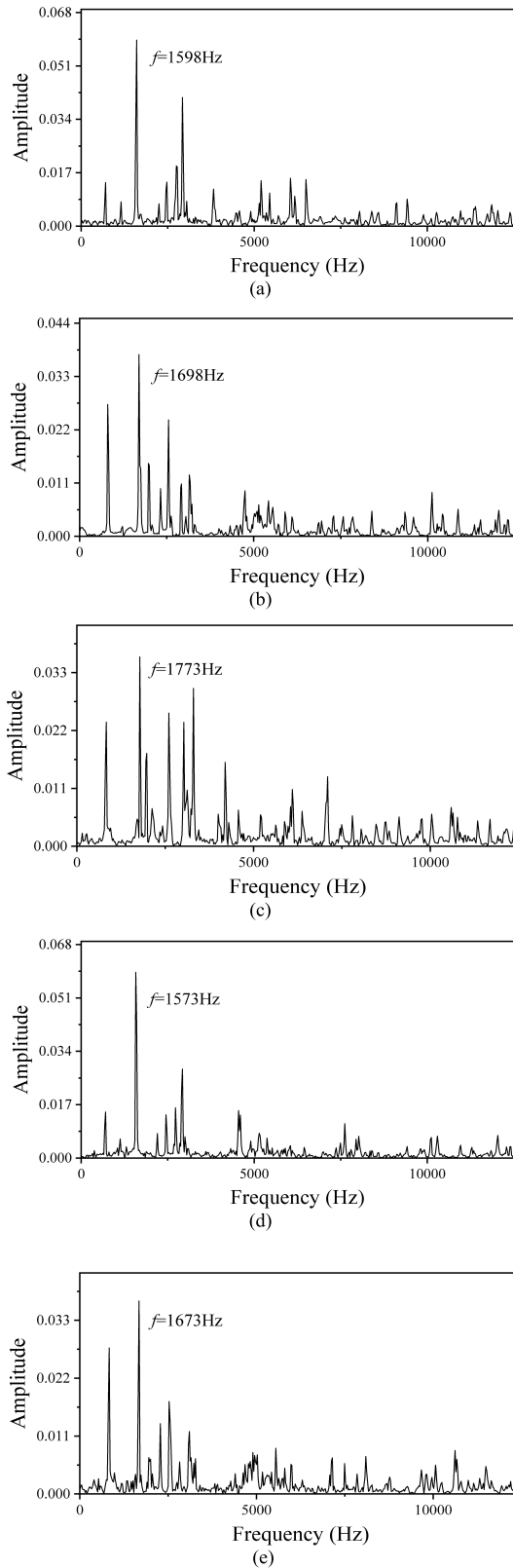


FIGURE 10. Frequency domain diagram of test points. (a) test point 2; (b) test point 3; (c) test point 4; (d) test point 5; (e) test point 6.

considered, it will not be enough to accurately calculate the thickness of multi-layer hearth. In order to reduce the error of

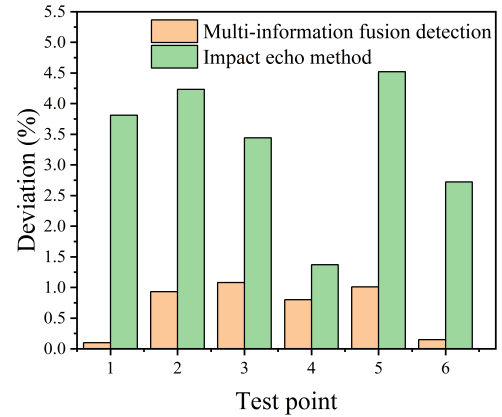


FIGURE 11. Temperature deviation diagram.

thickness calculation caused by wave velocity calibration of laboratory samples, it is necessary to calculate the influence of temperature of different material layers on wave velocity. At this time, detection of multi-information fusion can bring more accurate results of hearth lining thickness detection.

**B. CONSTRUCTION OF EROSION BOUNDARY**

The thickness values (Section III-A) and thermocouple data can be used to construct the erosion boundary under the hearth detection area. After comprehensive analysis, the erosion boundary model of hearth and bottom was constructed by cubic spline interpolation method [25], [26].

The steps of solving cubic spline curve are as follows. (1) According to the relationship between blast furnace hearth thickness and temperature obtained above, the equations satisfying the constraint conditions are listed. (2) According to the need, the boundary conditions of the endpoints can be determined, the interpolation fitting curve is obtained.

The temperature field solved by the erosion boundary model of hearth and bottom is shown in Fig. 12. The thickness of the uncovered position of the thermocouple on the model was detected by impact echo. At the same time, according to the node temperature of the cold surface of carbon brick below the test point, the corresponding thickness was obtained by interpolation. The impact echo thickness value was compared with the interpolation thickness, and the allowable deviation is 5% [27]. The test point is shown in Fig. 13.

The time-acceleration curve was obtained at the signal collection point and transformed into a frequency domain diagram by FFT. As shown in Fig. 14, there is an obvious peak at 1648Hz. The temperature factor of each material layer was calculated according to the temperature field in Fig. 12, and the cold surface temperature of carbon brick under the test point was 392.57°C. According to equation 7, the thickness of hearth lining carbon brick at the test point is 505.5mm. According to the interpolation calculation of temperature, the thickness is 516.7mm. The deviation between the two thickness results is 2.17%, which is less than 5% of the allowable deviation. In addition, the deviation between the calculated temperature of impact echo thickness and the interpolation temperature is also within the allowable error range.

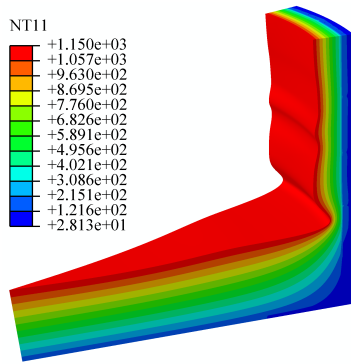


FIGURE 12. The temperature field.

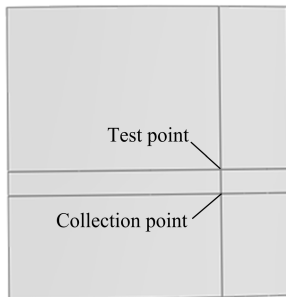


FIGURE 13. Location of test point and collection point.

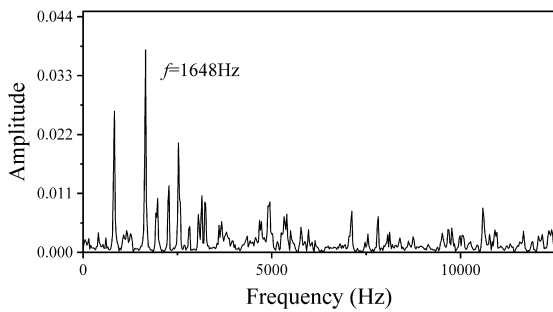


FIGURE 14. Frequency domain diagram of test point.

**C. THICKNESS CALCULATION OF IMPACT ECHO AND COOLING SYSTEMS**

The heat flux intensity in cooling stave refers to the heat flow per unit area of cooling stave per unit time. After the blast furnace starts production and reaches the predetermined technical indexes, the thermal working state of hearth cooling stave shows that the water temperature difference between inlet and outlet fluctuates in a relatively balanced range. Once the water temperature difference between inlet and outlet of cooling stave changes, it is shown that the water temperature difference is significantly different from the original steady state, and the original equilibrium is destroyed. For a certain part of the blast furnace hearth, there is a stable water temperature difference between the inlet and outlet of cooling stave. When the water temperature difference between inlet and outlet in the cooling stave pipe is in a relative equilibrium state, the heat flow can be considered as a constant during

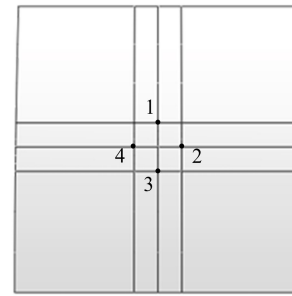


FIGURE 15. Grid division diagram of test points.

blast furnace smelting. Therefore, the heat flow can be calculated by the water temperature difference between inlet and outlet of the hearth cooling stave pipe, and then the interface temperature can be calculated.

According to the structure of blast furnace hearth, the temperature is calculated based on the long cylinder problem [28]. The water flow rate of the water pipe in the cooling stave was  $M_S = 2.51(\text{kg/s})$ , the temperature difference between inlet and outlet of single water pipe is  $\Delta T(^{\circ}\text{C})$ , the specific heat capacity of water is  $C_P = 4200[\text{J}/(\text{kg} \cdot \text{K})]$ , and the heat flow of the single cooling stave is  $Q_c(\text{W})$ .

$$Q_c = 4M_S C_P \Delta T \tag{10}$$

Thus, the heat flux  $q_c(\text{W}/\text{m}^2)$  on the cold surface of cooling stave is calculated as

$$q_c = \frac{Q_c}{2\pi r_c R B} \tag{11}$$

where,  $r_c$  is the radius of the cold surface of cooling stave,  $R$  is the radian of the cooling stave, and  $B$  is the height of the cooling stave.

According to convective heat transfer, the heat flux of the cold surface of the cooling stave is

$$q_{cT} = h_c(T_c - T_F) \tag{12}$$

where,  $T_F$  is the average temperature of cooling water,  $h_c$  is the equivalent convective heat transfer coefficient of the cold surface of cooling stave, and  $T_c$  is the temperature of the cold surface of cooling stave.

Set  $q_c = q_{cT}$ , the temperature  $T_c$  of the cold surface of the cooling stave can be obtained

$$T_c = T_F + \frac{q_c}{h_c} \tag{13}$$

The remaining interface temperatures can be solved by the convective heat transfer conditions at the outer boundary and equal conditions of heat flux [28].

The hearth is usually severely eroded in the later period of furnace service. So the detection is carried out at a certain hearth position, due to the influence of high temperature, high pressure, thermal stress and other factors, the thermocouple in this part was damaged. Therefore, the water temperature difference between the inlet and outlet of the cooling stave water pipe was measured, it is found that the temperature



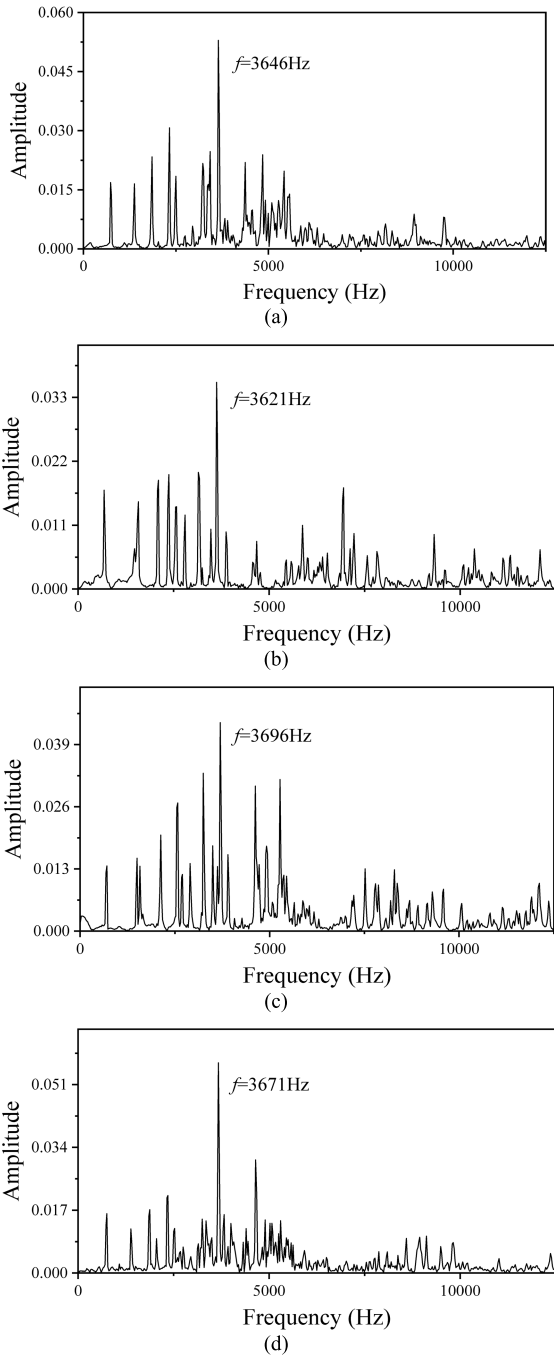


FIGURE 16. Frequency domain diagram. (a) test point 1; (b) test point 2; (c) test point 3; (d) test point 4.

difference between inlet and outlet of a cooling stave was obviously higher than that of other parts, it is judged that the carbon brick erosion under the cooling stave was more serious than other parts. And the temperature difference was 0.88°C. The interface temperature of each layer of hearth is shown in Table 6.

Due to the serious erosion of carbon brick in this hearth part, in order to reduce the error of single thickness measurement, the thickness of the local furnace hearth lining carbon brick was detected by a grid with an interval of 100mm.

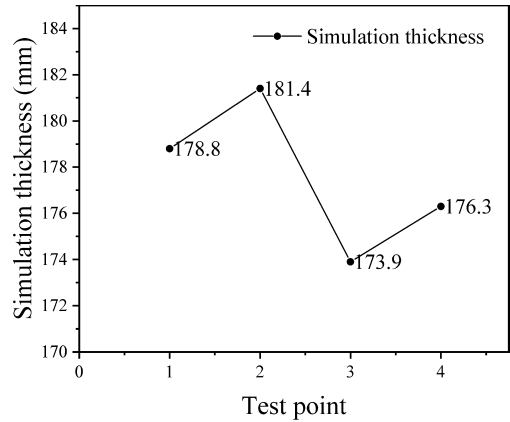


FIGURE 17. Simulation thickness results.

TABLE 6. Temperature calculation results of hearth.

Calculation parameter	Heat flow calculation	Multi-information detection	Difference (%)
Cold surface temperature of furnace shell(°C)	65.61	64.56	1.63
Hot surface temperature of furnace shell(°C)	66.32	65.26	1.62
Cold surface temperature of cooling stave(°C)	189.71	186.70	1.59
Hot surface temperature of cooling stave(°C)	265.32	263.75	0.59
Cold surface temperature of carbon brick(°C)	690.57	689.91	0.10

1, 2, 3 and 4 in Fig. 15 are the test points. According to the calculation principle, the frequency domain diagram of detection results was obtained at each test point, as shown in Fig. 16. According to the calculation equation of hearth thickness, the thickness of carbon brick at four test points is shown in Fig. 17.

According to the thickness of the above four test points, the average thickness of the carbon brick in the hearth is 177.6mm. Based on this thickness, the temperature field was calculated, and the node temperature of carbon brick cold surface is listed in Table 6. The relative difference between the two is solved, which is within the approved accuracy range and small.

According to the previous impact echo method, the wave velocity of carbon brick sample was calculated as 2700m/s. According to the thickness frequency in Fig. 16, the average thickness of carbon brick is 189.5mm. The temperature field of this thickness was calculated, and the node temperature of carbon brick cold surface was determined to be 671.97°C. The relative temperature difference is 2.69%. It can be seen that the thickness of carbon brick is calculated more accurately by multi-information fusion.

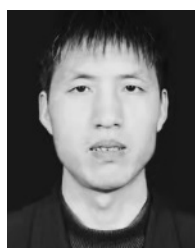
#### IV. CONCLUSION

In order to improve the accuracy of detecting the thickness of carbon brick in hearth lining by impact echo technology, taking the furnace hearth as the research object, we analyzed

a multi-information fusion detection method to determine the thickness of hearth lining carbon brick under different thermal parameters and different working conditions. Based on the multi-information fusion detection method, the node temperature of carbon brick cold surface solved by thickness result was verified by thermal parameters, which verifies the reliability and accuracy of thickness detection results. In addition, compared with the previous impact echo method, the results showed that the multi-information fusion method could detect the thickness of hearth lining carbon brick more accurately. This method provides a more accurate solution for the determination of hearth lining erosion.

## REFERENCES

- [1] Y. Ge, Y. Li, H. Wei, H. Nie, W. Ding, Y. Cao, and Y. Yu, "A novel approach for measuring the thickness of refractory of metallurgical vessels," *Materials*, vol. 13, no. 24, p. 5645, Dec. 2020.
- [2] A. Sadri, W. L. Ying, P. Gebiski, P. Szyplinski, T. Goff, and B. V. Beek, "A comprehensive review of acousto ultrasonic-echo (AU-E) technique for furnace refractory lining assessment," in *Proc. COM*, Quebec City, QC, Canada, 2015, pp. 23–26.
- [3] A. Sadri, "An introduction to stress wave non-destructive testing and evaluation (NDT&E) of metallurgical furnaces and refractory condition monitoring," *CINDE J.*, vol. 29, no. 2, pp. 7–11, 2008.
- [4] A. Sadri and P. Gebiski, "Monitoring refractory lining in operating furnaces by acousto ultrasonic-echo technique," presented at the 50th Conf. Metallurgists, Montreal, QC, Canada, Oct. 5, 2011.
- [5] A. Sadri and P. Gebiski, "Comparing the accuracy of acousto ultrasonic-echo (NDT), finite element analysis (FEA), and drilling when obtaining a blast furnace refractory lining wear profile," in *Proc. AISTech*, St. Louis, MO, USA, 2009, pp. 272–287.
- [6] A. Sadri, P. Gebiski, and E. Shameli, "Refractory wear and lining profile determination in operating electric furnaces using stress wave non-destructive testing (NDT)," in *Proc. INFACON*, Helsinki, Finland, 2010, pp. 881–890.
- [7] S. V. Filatov, I. F. Kurunov, Y. M. Gordon, D. N. Tikhonov, and S. N. Grachev, "Extending the campaign life of an intensively operating blast furnace," *Metallurgist*, vol. 60, nos. 9–10, pp. 905–911, Jan. 2017.
- [8] E. Vinogradov, M. Karimov, Y. Gordon, A. Sadri, and N. Spirin, "Use of non-distractive testing AU-E technology to evaluate hearth conditions at CherMK-SEVERSTAL," in *Proc. KnE Eng.*, Moscow, Russian, 2018, pp. 57–70.
- [9] A. Sadri, S. Filatov, I. Kurunov, Y. Gordon, W. L. Ying, and J. Erskine, "Monitoring and control of refractory wear for intensive operation of blast furnace," in *Proc. ABMDA*, Rio de Janeiro, Brazil, 2016, pp. 191–201.
- [10] H. Ghorbani, M. Al-Dojayli, and K. Chomyn, "Thermal assessment and identification of wear zones in a blast furnace hearth and tap-holes," in *Proc. SAIMM*, Cape Town, South Africa, 2018, pp. 39–48.
- [11] M. O. Zolotikh, A. N. Dmitriev, and G. Y. Vitkina, "The association of various approaches to the monitoring of lining condition in the blast furnace hearth," *Defect Diffusion Forum*, vol. 380, pp. 186–190, Nov. 2017.
- [12] L. Yu, "Thermal state model and lining erosion identification of blast furnace hearth," (in Chinese), Ph.D. dissertation, School Mech. Eng. Automat., Northeastern Univ., Shenyang, China, 2009.
- [13] F. M. White, *Fluid Mechanics*, M. Lange, Ed., 2nd ed. New York, NY, USA: McGraw-Hill, 2009.
- [14] L. Y. Chen and Y. Li, "Convective heat transfer boundary equivalent replacement and model simplification of cooling stove of blast furnace hearth," *Res. Iron Steel*, vol. 35, no. 6, pp. 26–29, Dec. 2007.
- [15] X. G. Ma, "Simulation and optimization study on thermal-mechanical coupling characteristics of middle and lower structure of blast furnace under the heating and opening conditions," (in Chinese), Ph.D. dissertation, School Mech. Eng. Automat., Northeastern Univ., Shenyang, China, 2018.
- [16] N. J. Carino, "Impact echo: The fundamentals," presented at the CNDT-CE Int. Symp., Berlin, Germany, Sep. 2015.
- [17] A. Sadri and R. Timmer, "Blast furnace non-destructive testing (NDT) for defect detection and refractory thickness measurements," in *Proc. AISTech*, Cleveland, OH, USA, 2006, pp. 593–602.
- [18] V. Kushnarev, K. Mironov, Y. Gordon, A. Sadri, W. Ying, and S. A. Zagainov, "AU-E control of blast furnace refractory lining at NTMK-Evraz ensures intensive operation and prediction of the end of campaign of titania blast furnace," presented at the ESTAD, Vienna, Austria, Jun. 29, 2017.
- [19] A. Sadri, M. Lachemi, and G. Walters, "Determination of refractory lining thickness and quality in operating industrial furnaces using a stress wave reflection technique," in *Proc. 1st CSCE*, Toronto, ON, Canada, 2005, pp. 1–10.
- [20] Y. M. Gordon, A. Sadri, K. V. Mironov, and N. A. Spirin, "Diagnostics of blast-furnace linings," *Steel Transl.*, vol. 47, no. 8, pp. 517–522, Aug. 2017.
- [21] A. Sadri, W. L. Ying, J. Erskine, and R. Macrosty, "Smelting furnace non-destructive testing (NDT) and monitoring," in *Proc. 19th WCNDT*, Munich, Germany, 2016, pp. 1–12.
- [22] C.-Y. Wang, C.-L. Chiu, K.-Y. Tsai, P.-K. Chen, P.-C. Peng, and H.-L. Wang, "Inspecting the current thickness of a refractory wall inside an operational blast furnace using the impact echo method," *NDT & E Int.*, vol. 66, pp. 43–51, Sep. 2014.
- [23] A. Sadri, P. Gebiski, and Y. Gordon, "Non-destructive testing (NDT) and inspection of the blast furnace refractory lining by stress wave propagation technique," in *Proc. 5th ICSTI*, Mississauga, ON, Canada, 2010, pp. 951–955.
- [24] A. Sadri, I. Gordon, and A. Rampersad, "Acousto ultrasonic-echo (AU-E): A non-destructive testing technique for blast furnace hearth refractory condition monitoring," in *Proc. AdMet*, Dnipropetrovsk, Ukraine, 2007, pp. 77–85.
- [25] H. Anton and C. Rorres, *Elementary Linear Algebra*. New York, NY, USA: Wiley, 2010.
- [26] D. Hanselman and B. Littlefield, *Mastering MATLAB 6: A Comprehensive Tutorial and Reference*. Englewood Cliffs, NJ, USA: Prentice-Hall, 2001, pp. 259–273.
- [27] S. Lee, N. Shin, and Y. Roh, "Estimation of the thickness of refractory ceramics using the impact-echo method," *J. Acoust. Soc. Korea*, vol. 36, no. 4, pp. 247–253, Jul. 2017.
- [28] S. Biswas and D. Sarkar, *Introduction to Refractories for Iron- and Steel-making*, 1st ed. Cham, Switzerland: Springer, 2020, pp. 182–184.



**JIAOCHENG MA** was born in Shanxi, China, in 1979. He received the B.Eng. and M.Eng. degrees in mechanical engineering and the Ph.D. degree in detection technology and automation device from Northeastern University, Shenyang, China, in 2002, 2005, and 2009, respectively. He is currently an Associate Professor with the School of Mechanical Engineering and Automation, Northeastern University. He has authored more than 20 articles. His research interests include embedded design, virtual instrument development, and complex process parameter detection, modeling, and optimization control.



**XUEWEI WEN** was born in Hebei, China, in 1995. He received the B.Eng. degree in mechanical engineering from the Liaoning University of Technology, Jinzhou, China, in 2018. He is currently pursuing the M.S. degree in mechanical engineering with Northeastern University, Shenyang, China. His research interest includes thickness detection of blast furnace.



**XIN ZHAO** received the M.S. and Ph.D. degrees in mechanical engineering from Northeastern University, Shenyang, China, in 2005 and 2014, respectively. He is currently a Senior Engineer with the Liaoning Provincial Institute of Safety Science. His current research interests include lifting machinery safety technology inspection, reliability analysis, and fault diagnosis.

...